# The Waves Michelson Interferometer: Design Principles and Validation

Valérie Losier[1], Dennis Arsenault[1], Jeffery Langille[1] and William Ward[1]

1. Department of Physics, University of New Brunswick, Fredericton, Canada

## Introduction

The Waves Michelson Interferometer (WaMI) is a new approach to the Michelson interferometer intended to simultaneously measure dynamical signatures, such as wind and temperature, and constituent signatures in the upper stratosphere, mesosphere and lower thermosphere (from 45 to ~180 km). From observation, the large scale circulation and dynamics is more complex than the models predict. This spectral imaging by the satellite instrument will allow to investigate the fundamental physics of the coupling of waves in the atmosphere and provide guidance to the existing models.

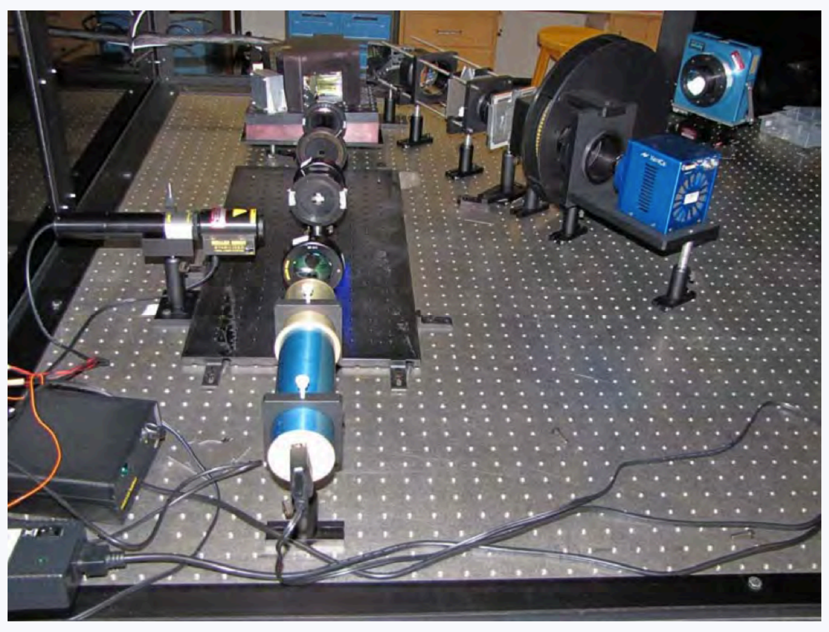

***Figure 1:*** *Photo of WaMI at the University of New Brunswick, NB*

## Objectives

Atmospheric motion results in a Doppler shift in the wavelength of the observed emission lines. For WaMI, these include lines in the molecular oxygen infrared bands, hydroxyl bands and the oxygen green line. The associated shift in the fringe phase allows wind to be established. The remaining fringe parameters allow constituent information (from the irradiance) and temperature (relative irradiance and visibility) to be determined.

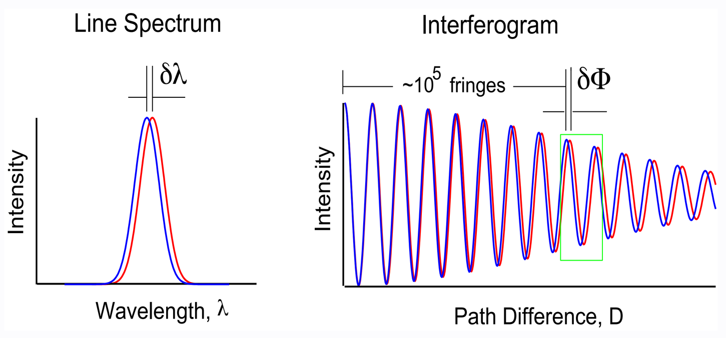


***Figure 2:*** *Doppler shift and the effect on the wavelength and its Fourier transform.*

## Michelson Interferometer

The moving mirror at the extremity of the gap is mounted on piezoelectrics that are controlled through a capacitative position sensor. Using the graphical user interface, MALICE, designed by COMDEV, a current can be sent to each piezo which then changes its length and consequently changes the gap size and tilt of the mirror.

The radiance on a small area at a particular interferometer phase can be expressed as

$$I_{\Omega I} = I_B + \sum F_I^l R_I^l \int_\Omega E^l(s) T^l(s)[1 + U_I^l V^l(s)\cos(\Phi_I^l + \phi_w(s))]ds$$

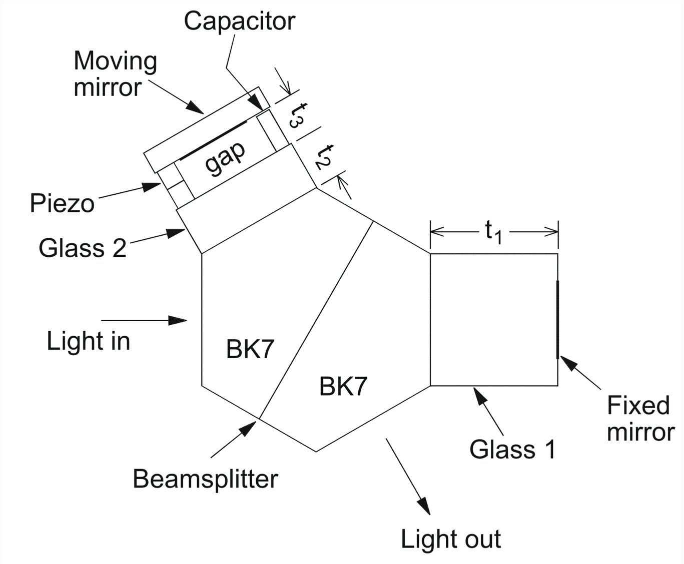


***Figure 3:*** *Scale drawing of the interferometer.*

### Wide angle

The rays emerge co-linearly due to the refractive material resulting in a slow change in phase over the field of view.

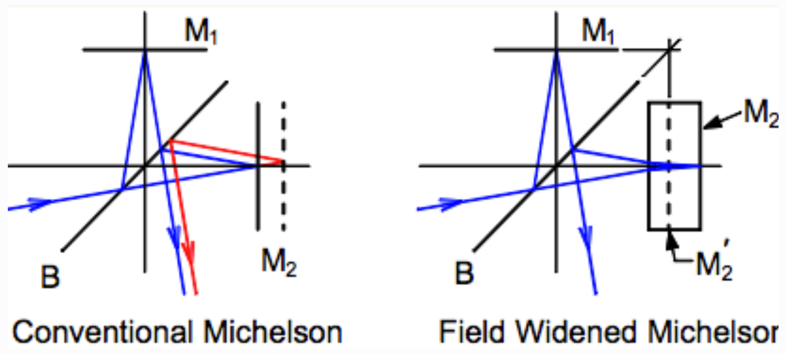


***Figure 4:*** *The conventional and field-widened Michelson Interferometer*

### Segmented mirror

The phase steps deposited on the back mirror allows for simultaneous fringe sampling at different optical paths.

The summation of two images 180 degrees out of phase yields an irradiance image. This feature minimizes the aliasing of atmospheric intensity variations into the fringe parameter determinations.

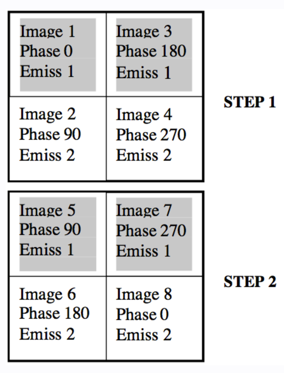


***Figure 5:*** *The quadrant phases*

## Optical Configuration

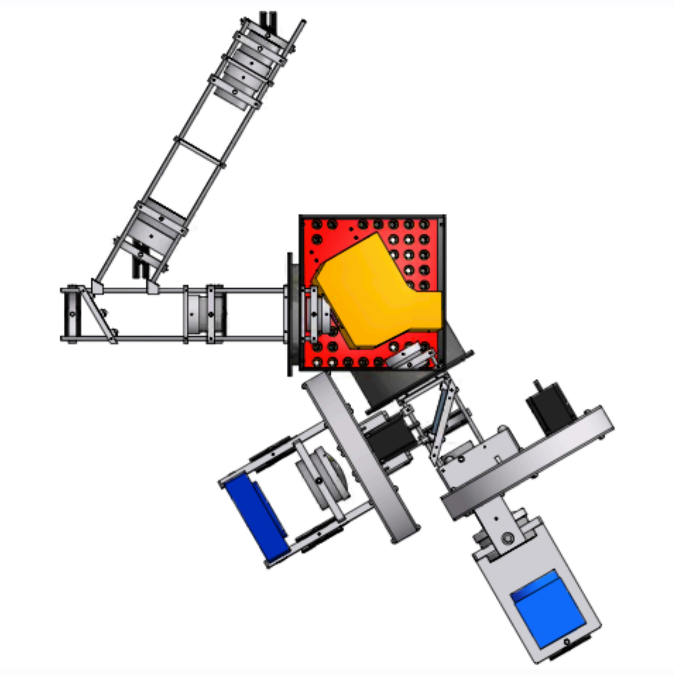

***Figure 6:*** *Design of the optical system*

WaMI is set up to take simultaneous measurements from both its visible and near infrared channel.

### Visible channel

The reflected emissions from the dichroic filter are the green and the hydroxyl line.
The channel is equipped with a prism which deviates the light of each quadrant by an angle D and the quadrants are imaged separately.

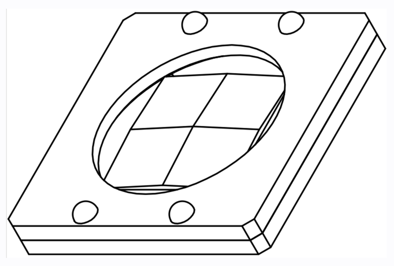

***Figure 7:*** *Sketch of the prism*

### Near infrared channel

| Emission | Line | Wavelength in air, λ (nm) |
|---|---|---|
| $O_2$ $^1\Delta$ (0,0) strong | $^RQ(9)$ | 1264.060 |
| | $^SR(3)$ | 1264.277 |
| | $^RR(9)$ | 1264.386 |
| $O_2$ $^1\Delta$ (0,0) weak | $^PQ(19)$ | 1278.289 |
| | $^OP(11)$ | 1278.408 |
| | $^PP(19)$ | 1278.590 |
| OH (8,5) | $P_1(4)$ | 1315.682 |
| O ($^1S$) | | 557.73 |

***Table 1:*** *Emission lines for WaMI*

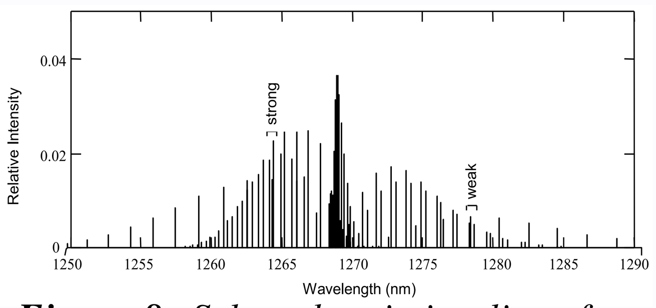


***Figure 8:*** *Selected emission lines from the $O_2$ molecular band*

The relative intensity of the selected emission lines can be used obtain the rotational temperature.

The lines were chosen using the following criteria:

- They are optically isolated
- The difference in the line strengths is close to one order of magnitude
- Each set contains lines from two different branches within the band

A Fabry-Pérot etalon separates the emission lines to be imaged.

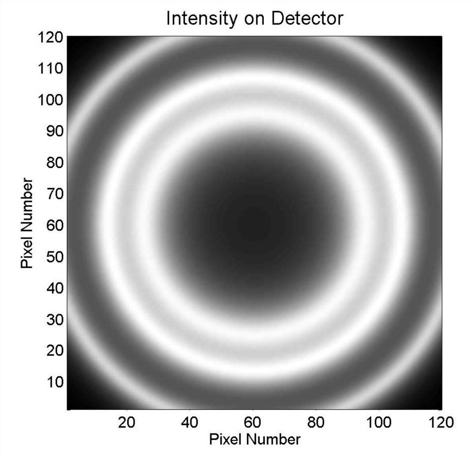


***Figure 9:*** *Simulated image of $O_2$ strong lines*

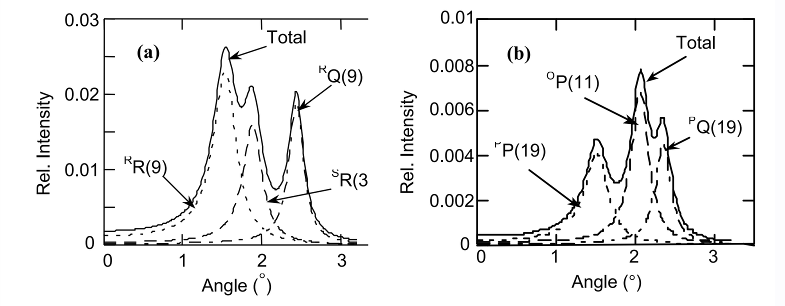


***Figure 10:*** *Relative intensity as a function of incident angle seen through the etalons for the (a) strong and (b) weak $O_2$ lines*

## Validation

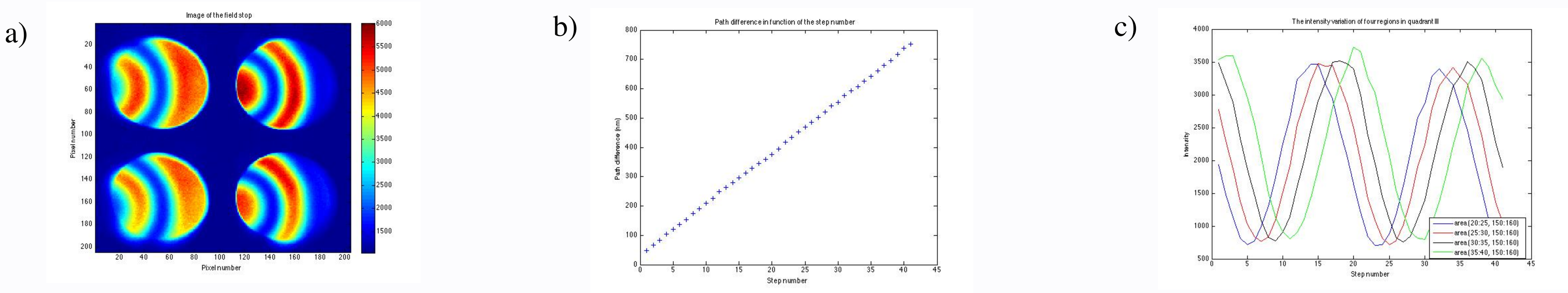


***Figure 11:*** *Results from imaging the field stop in the visible channel using a helium-neon laser source and running a MATLAB program on the data. a) Image form the CCD b) The path difference at each step c) The variation of intensity at four chosen points in the third quadrant*

Figure 11 a) shows the contrast in intensity between minima and maxima. The visibility can be estimated using the visibility equation $V = \frac{I_{max} - I_{min}}{I_{max} + I_{min}}$

Stepping the interferometer moves the back mirror without changing its tilt therefore the fringes are displaced radially and move through the field of view. Imaging 41 steps and running the pixel values of chosen areas in a MATLAB program calculates, among other parameters, the visibility of each area. After aligning the instrument, the average visibility was 0.7.

Figure 11 b) shows that from the phase and path difference relationship, $\Delta d = \frac{\lambda \Delta \phi}{4\pi}$, we confirm with the phase information that the increase in the gap size is consistent and linear.

Figure 11 c) shows that each area chosen on the third quadrant goes through the same intensity variation, as predicted by interferometer equation. It is simply shifted in time.

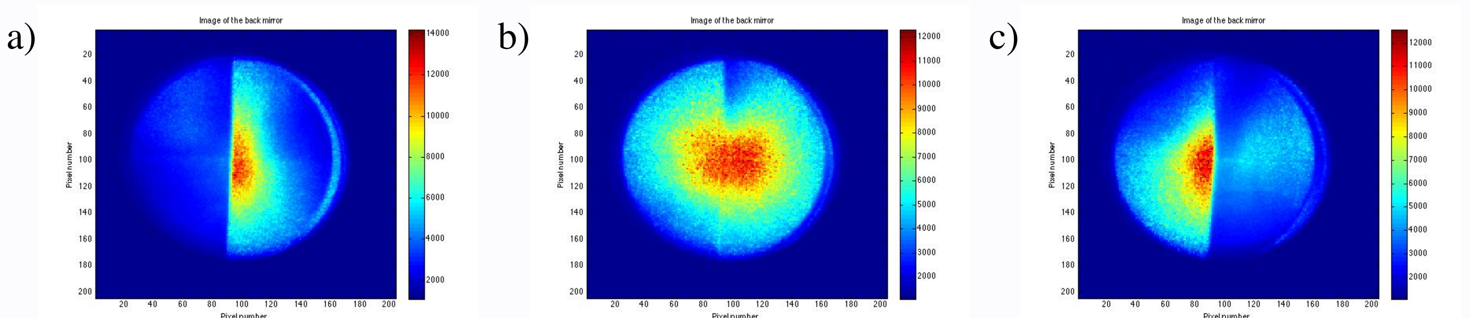


***Figure 12:*** *Imaging the straightened back mirror. a) First image b) Image after 3 steps c) Image after 6 steps*

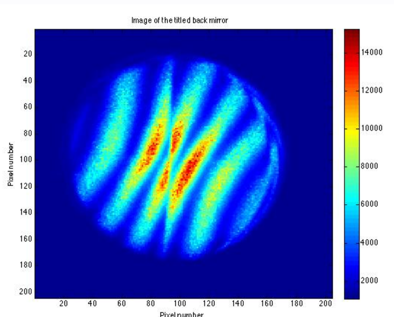

***Figure 13:*** *Imaging a titled back mirror*

An optical system is set up to image the mirror and look at the fringes of equal thickness. If the mirror is tilted, there will be fringes, as shown in figure 13. The MALICE system is used to straighten the mirror. Displacing the mirror back and forth should not reveal fringes of equal thickness. The phase gradient can be obtained from imaging consecutive steps.

## Conclusion and Future Work

Validation for a few WaMI principles have begun using the methods previously mentioned. Further validation for other aspects of the instrument is underway such as the four quadrant system and the principle of using multiple emission lines in order to obtain information on temperature of the atmosphere. Since the phase steps deposited on the back mirror were not 90 degrees out of phase as needed, the manufacturing company will be asked to make a new mirror. The next step will be to use a realistic source to validate the WaMI principles. It will then also be set up as a field instrument to image only the visible green and hydroxyl lines, since molecular oxygen is typically absorbed as it looses altitude.

## Acknowledgements

Instruments supplied by COMDEV and light LigthMachinery. This work is supported by the Canadian Network for the Detection of Atmospheric Change (CANDAC) and its funding partners: Canadian Space Agency; Canadian Foundation for Innovation; Environment Canada, Meteorological Service of Canada; Ontario Innovation Trust; Canadian Foundation for Climate Change and Atmospheric Science; Polar Continental Shelf Program; Ontario Ministry of Research and Innovation; Natural Sciences and Engineering Research Council of Canada; Government of Canada IPY funding; Study of Environmental Arctic Change; and the Nova Scotia Research and Innovation Trust.
A special thank you to the Collaborative Research and Training Experience Program (CREATE), the department of physics at the University of New Brunswick and to Professor William Ward, Samuel Kristoffersen and Jeffery Langille for their help and support throughout the project.

## References

Gordon G Shepherd. *Spectral Imaging of the Atmosphere*. vol. 82 of the AP International Geophysics Series. London, UK: Academic Press, 2002.
William E. Ward et al. (2010), Final Report on the Advanced Study: Dynamics and Constituent Transport from the Stratosphere to the Thermosphere - The Enhanced Waves Michelson Interferometer
Eugene Hecht. *Optics*. fourth edition. Addison-Wesley Longman, Inc., 2002.

For further information, please contact: valerie.losier@mail.mcgill.ca